Applied Environmental Microbiology Core: Rapid Deduction of Stress Response Pathways in Metal/Radionuclide Reducing Bacteria

Terry C. Hazen*[1], Carl Abulencia[3], Gary Anderson[1], Sharon Borglin[1], Eoin Brodie[1], Steve van Dien[7], Matthew Fields[6], Jil Geller[1], Hoi-Ying Holman[1], Richard Phan[1], Eleanor Wozei[1], Janet Jacobsen[1], Dominique Joyner[1], Romy Chakraborty[1], Martin Keller[2], Aindrila Mukhopadhyay[1], David Stahl[5], Sergey Stolyar[5], Judy Wall[4], Huei-che Yen[4], Grant Zane[4], Jizhong Zhou[2,7], E. Hendrickson[5], T. Lie[5], J. Leigh[5], Chris Walker[5]

1. E. O. Lawrence Berkeley National Laboratory, 2. Oak Ridge National Laboratory, 3. Diversa, Inc., 4. University of Missouri, Columbia, 5. University of Washington, 6. Montana State University, 7. University of Oklahoma

http://vimss.lbl.gov/

INTRODUCTION

AEMC of the ESPP project is the source of environmental data and samples that determine the stressors that will be studied, provides the environments for growing the organisms to be tested, simulates stressed environments, and verifies the conceptual models to determine how these stress regulatory pathways control the biogeochemistry of contaminated sites

Field Studies

Groundwater bacterial communities were monitored in several wells along a transect that were stimulated via the addition of a potential electron donor (i.e., ethanol). Electron donor was added intermittently over 650 days. By day 535, the nitrate levels in the groundwater had decreased from 10 mM to 0.5 mM, and groundwater uranium levels had declined from approximately 2 mg/l to 0.2 mg/l. Bacterial community composition and structure were characterized via clonal libraries of the SSU rRNA gene sequences. The up-stream and injection well had similar diversity indices, whereas the treatment zone and immediately down-stream well both had increased diversity. When the entire sequence libraries were compared via LIBSHUFF analysis. The results indicated that the bacterial community composition and structure changed upon bio-stimulation for metal-reducing conditions, and that sequences indicative of *Anaeromyxobacter* and *Desulfovibrio* were detected in wells that displayed a decline in both nitrate and uranium upon bio-stimulation. The results also suggested that, in addition to the presence of desired populations, an increase in diversity may be important for optimal functionality.

Site	Predominant Clones	Clones of Interest	Sample Type
FW-005	*Azoarcus* ; *Pseudomonas* ; *Ralstonia*		Groundwater
FW-024	*Zoogloea* ; *Dechloromonas* ; α - Prot.		Groundwater
FW-104	*Zoogloea* ; *Thauera* ; *Ferribacterium*		Groundwater
FW-101	*Acidovorax* ; *Ferribacterium*	*Desulfovibrio* ; *Anaeromyxobacter*	Groundwater
FW-026	*Acidovorax* ; *Ferribacterium*	*Desulfovibrio*	Groundwater
FW-103	*Zoogloea* ; *Ferribacterium*	*Desulfovibrio*	Groundwater
FW-109	*Anaeromyxobacter*	*Anaeromyxobacter*	Sediment Enrichment

During Stimulation- day 535

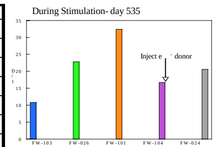

Relationship Between Sites Based Upon Clonal Libraries

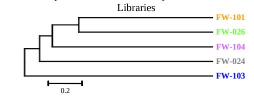

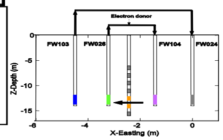

[13]C-labelled lactate was injected in August 2004 at the Hanford 100H site to biostimulate chromium reduction. After more than 1 year chromium was still at non-detect in the stimulated wells. 16s phylochip analyses showed a dramatic increase in diversity at the stimulated wells, including iron reducers (*Geobacter*) and sulfate reducers (*Desulfovibrio*). Sequentially competing terminal electron acceptors were depleted: oxygen, nitrate, iron(III), and sulfate. [13]C was detected in the dissolved inorganic carbon and in the signature lipids (PLFA) of iron reducers and sulfate reducers. Sulfate reduction was still active after more then a year in the deepest parts of the aquifer, and iron(II) still dominated suggesting an active Cr(IV) reducing environment. *Desulfovibrio* strains have been isolated and are currently being sequenced. Stress responses in these strains will be compared to the pipeline studies on DvH already completed.

Metagenome Analysis of FRC Sediment (Biopanning/MDA)

Table 4. Cog analysis

Function classification	Area 3, Deep		Area 3, Shallow		Area 2	
	No. of sequences	%	No. of sequences	%	No. of sequences	%
Amino acid transport and metabolism	64	4.0558	47	4.1337	75	4.6325
Carbohydrate transport and metabolism	187	11.8504	184	16.1829	232	14.3298
Cell cycle control, cell division, chromosome partitioning	16	1.0139	11	0.9675	21	1.2971
Cell motility	4	0.2535	4	0.3518	7	0.4324
Cell wall/membrane/envelope biogenesis	117	7.4144	88	7.7397	122	7.5355
Coenzyme transport and metabolism	68	4.3093	23	2.0229	31	1.9148
Defense mechanisms	42	2.6616	28	2.4626	43	2.656
DNA replication, recombination and repair	85	5.3866	61	5.365	84	5.1884
Energy production and conversion	216	13.6882	162	14.248	246	15.1946
Function unknown	117	7.4144	47	4.1337	67	4.1384
General function prediction only	119	7.5412	100	8.7951	130	8.0296
Inorganic ion transport and metabolism	88	5.5767	57	5.0132	44	2.7177
Intracellular trafficking, secretion, and vesicular transport	12	0.7605	12	1.0554	15	0.9265
Lipid transport and metabolism	36	2.2814	12	1.0554	22	1.3589
Nucleotide transport and metabolism	30	1.9011	21	1.847	47	2.903
Posttranslational modification, protein turnover, chaperones	190	12.0406	146	12.8408	196	12.1062
RNA processing and modification	1	0.0634		0	3	0.1853
Secondary metabolites biosynthesis, transport and catabolism	26	1.6477	21	1.847	13	0.803
Signal transduction mechanisms	80	5.0697	31	2.7265	91	5.6208
Transcription	37	2.3447	30	2.6385	47	2.903
Translation, ribosomal structure and biogenesis	43	2.725	52	4.5734	83	5.1266
Total	1578		1137		1619	

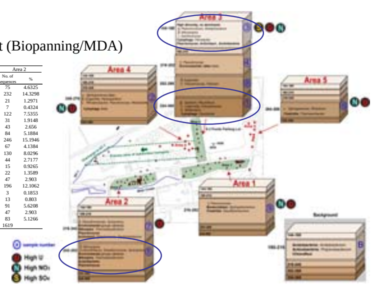

Extremely toxic environment
- pH - 3.7
- Uranium - 51 mg/L (soil ~500 mg/kg): with the highest U contamination in the world
- Nitrate Š 2,331 mg/L

Metagenomic sequencing:
- Almost like a mono-culture
- 52.44 Mb raw data assembled into contigs totaling ~5.5 Mb
- 224 scaffolds (largest 2.4 Mb)
- Genes important to the survival and life style in such environment were found

Extremely low diversity:
- Dominated by *Frateuria* -like organism
- At least 2 *Frateuria* phylotypes
- Azoarcus species: less abundant

These results suggest that contaminants have dramatic effects on the groundwater microbial communities, and these populations are well adapted to such environments.

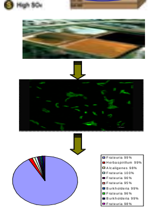

FRC Groundwater Metagenome Analysis

DUAL CULTURE SYSTEMS

How does *Desulfovibrio vulgaris* cooperate with other organisms to grow without sulfate?

To understand this question, we have engineered a syntrophic association between *D. vulgaris* and *Methanococcus maripaludis* such that *D. vulgaris* can grow and degrade lactate in the absence of sulfate (Figure 1). We have been investigating the physiology of this interaction by:

A. Characterizing growth, metabolic activity, and metabolite fluctuations through all stages of growth in a batch culture environment (Figure 2).

B. Utilizing genomic and physiological data about each organism to construct a stoichiometric metabolic model (Figure 3).

C. Compared gene expression of each organism grown in coculture with its expression in mono-culture to determine which genes and pathways are necessary for coculture growth (Figure 4).

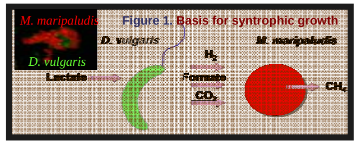

Figure 1. Basis for syntrophic growth

Figure 2. Growth and metabolite evolution in syntrophic coculture.

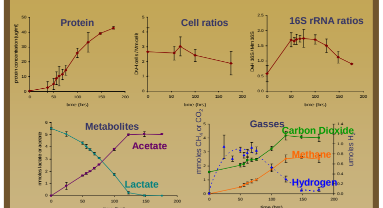

Protein concentration (A), Ratio of *D.vulgaris* to *M. maripaludis* cells over time, determined from microscopic cell counts (B), Relative abundance of 16S rRNA for each species measured by capillary electrophoresis on an Agilent Bioanalyzer (C), mmoles of metabolites (D) and gasses (E) produced and consumed over time. Data points indicate the mean of four independent cultures and error bars indicate the bounds of 95% confidence intervals.

- Analysis of growth, metabolic activity, and fluctuations of metabolites demonstrates conversion of lactate into acetate and methane by the co-culture as predicted.
- The activity of the two species is not coupled over time as may be suggested by the thermodynamic couplings between the metabolic reactions that each performs. Rather, *D. vulgaris* is more active in the early stages of consumption of lactate, while *M. maripaludis* is relatively more active after the hydrogen concentration has peaked. These non-synchronous growth dynamics are evident in the ratio of 16S rRNA abundance for each species and the linear rather than logarithmic growth dynamics.

Figure 3. Diagram of stoichiometric model.

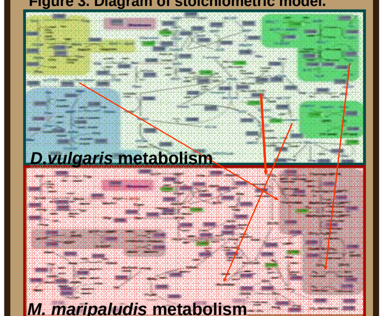

Boxes indicate predicted flux rates for each reaction in umol/hr in an example simulation. Biomass flux is given in grams dry cell weight / hr. Red arrows indicate components that the model predicts are exchanged between species in the coculture

- The flux-balance model predicts that either hydrogen or formate may be used as electron carriers (see red arrows) in this interaction. However, a formate dehydrogenase deficient *M. maripaludis* mutant is able to grow in the syntrophic conditions, indicating that formate metabolism is not necessary for syntrophic growth with *D. vulgaris*. Future experiments will address whether there are quantitative effects on syntrophic growth of the ability to metabolize formate.

Figure 4. Visualization of microarray data overlaid on *D. vulgaris* metabolic pathway model

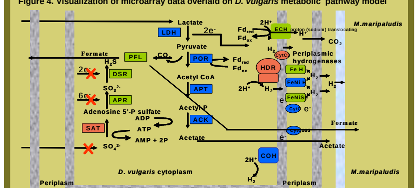

Colored shapes represent proteins. [red] indicates upregulation, [blue] downregulation, and [green] no change in gene expression in co-culture. ✕ indicates absence of a flux through the sulfate reduction pathway (DvH is not reducing sulfate in the co-culture environment). DSR – dissimilatory sulfite reductase; APR – APS reductase; SAT – sulfate adenyl transferase; LDH – lactate dehydrogenase; POR –Pyruvate ferredoxin oxidoreductase; APT – acetyl P transferase; ACK - acetate kinase; HDR – heterodisulfide reductase (hydrogenase); ECH – energy conserving hydrogenase; Fe H – Fe containing hydrogenase; FeNi H – Fe Ni containing hydrogenase; FeNiSe – Fe Ni and selenocysteine containing hydrogenase; COH – CO induced hydrogenase; Cyt – cytohrome; PFL – pyruvate formate lyase

- Even though *D. vulgaris* is fermenting lactate to acetate in the co-culture medium, genes involved in catabolism of lactate to acetate seem to be downregulated.
- Genes for the sulfate reduction pathway were still expressed in the absence of sulfate.
- Several hydrogenases were downregulated reflecting changes in energy producing pathways
- *M. maripaludis* gene expression results suggest upregulation of a gene coding for a formate transporter (data not shown), suggesting that reducing power is being exchanged between the species *via* formate in addition to hydrogen.

Figure 5. Metabolite flux rates for syntrophic growth predicted by FBA compared to experimental data.

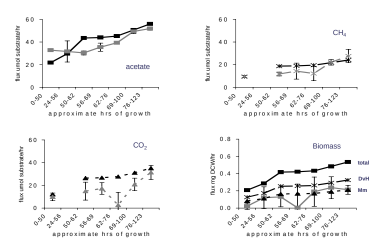

Black – predictions; Grey – experimental data

Enrichments from contaminated sites

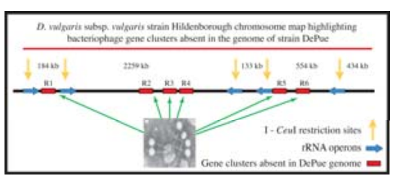

- *D. vulgaris* strain DePue lacks bacteriophage associated with strain Hildenborough
- Genome sequencing of strain DePue underway at the JGI
- Isolation of sulfate-reducers from Hanford Site 100-H Area field site currently under way

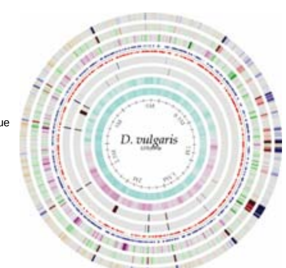

PIPELINE EXPERIMENTS

High Throughput Biomass Production.

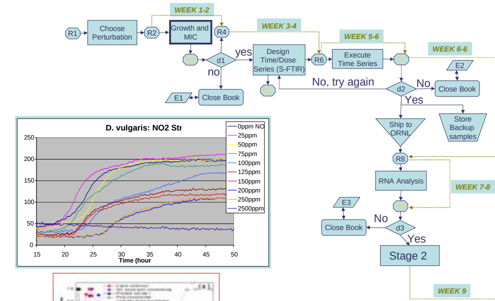

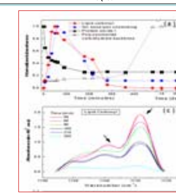

Synchrotron FTIR Spectromicroscopy for Real-Time Stress Analysis. By comparing measurements, we were able to identify tight temporal changes in chemical bonds, functional groups, and chemical substructures in lipids, DNA, proteins, and polyglucose in *D. vulgaris*. For example, when exposed to moderate concentrations of O_2 or NO_3, *D. vulgaris* increases the production of exopolysaccharides but with little change in protein structures. However, when exposed to moderate concentration of NaCl, *D. vulgaris* again increases the production of exopolysaccharides while exhibiting a significant change in protein structures. These studies also enabled focusing of VIMSS transcriptomic, proteomic, and metabolomic studies on the best time points to rapidly resolve stress response pathways

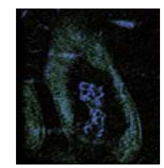

A plastic-embedded section of *Desulfovibrio vulgaris* prepared after brief exposure to air. Left: A micrograph of the section, which was about 300 nm thick shows two cells, one a the left cut in cross section and one the right nearly longitudinally. Right: A slice through the 3-D reconstruction shows partially condensed nucleic acid and non-staining region toward the middle of the cell surrounded by a denser region with limited structure. K. Downing & H.-Y. Holman

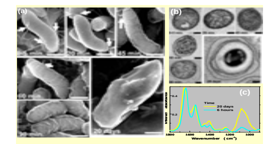

Phenotypic Microarray™ In the last year we have further refined our phenotyping of DvH to minimize the number of plates necessary. We have also screened 15 knockout mutants of DvH and 10 knockout mutants of *Shewanella* MR1. See (https://vimss.lbl.gov/~jsjacobsen/cgi-bin/Test/HazenLab/Omnilog/home.cgi) for sample data sets and analyses.

PUBLICATIONS FY06

ACKNOWLEDGEMENT

ESPP is part of the Virtual Institute for Microbial Stress and Survival supported by the U. S. Department of Energy, Office of Science, Office of Biological and Environmental Research, Genomics:GTL Program through contract DE-AC02-05CH11231 between Lawrence Berkeley National Laboratory and the U. S. Department of Energy.